40th Fluid Dynamics Conference and Exhibit
28 June - 1 July 2010, Chicago, Illinois

AIAA 2010-5026

# Dynamic k-Equation Model for Large Eddy Simulation of Compressible Flows

Xiaochuan Chai * and Krishnan Mahesh †
*University of Minnesota, Minneapolis, MN, 55455, USA*

**This paper presents a new dynamic one equation eddy viscosity model for LES of compressible flows. Based on the compressible version of dynamic Smagorinsky model (DSM), the transport equation for sub-grid scale (SGS) kinetic energy (KE) is introduced to predict SGS KE, instead of the commonly used Yoshizawa's model. The SGS KE transport equation for compressible flow is derived, and the unclosed terms in the compressible energy equation are modeled and dynamically closed using the Germano identity. The proposed model is then incorporated into the parallel finite volume Navier-Stokes solver on unstructured grids developed by Park & Mahesh (2007) and applied to decaying isotropic turbulence and normal shock/isotropic turbulence interaction.**

## Nomenclature

| | | |
|---|---|---|
| $k$ | = | Sub-grid scale kinetic energy |
| $\tau_{ij}$ | = | Sub-grid scale stress tensor |
| $\sigma_{ij}$ | = | Viscous stress tensor |
| $S_{ij}$ | = | Rate of strain tensor |
| $\delta_{ij}$ | = | Kronecker delta |
| $R$ | = | Specific gas constant |
| $C_p$ | = | Specific heat at constant pressure |
| $\mu$ | = | Viscosity |
| $Pr$ | = | Prandtl number |
| $\lambda$ | = | Taylor micro scale |
| $\epsilon$ | = | Dissipation |
| $M$ | = | Mach number |
| $Re$ | = | Reynolds number |

## I. Introduction

Large-eddy simulations directly calculate the large-scale motions of the flow fields from the filtered Navier-Stokes equations, and model the unresolved motions. The dynamic Smagorinsky model (DSM), introduced by Germano *et al.*,[1] has been successfully applied to the LES of incompressible flows. It provides a systematic method (Germano identity) of obtaining the closure coefficient $C_s$ in the Smagorinsky's eddy viscosity model.[2] Moin *et al.*[3] extended the DSM model to compressible flows. Different from incompressible flows, the sub-grid scale kinetic energy has to be modeled explicitly. For compressible LES, Moin *et al.* use Yoshizawa's model[4] for SGS KE. However, it is well known[5,6] that Yoshizawa's model tends to under-predict the magnitude of SGS KE. Obtaining the SGS KE from its transport equation has shown

*Graduate Research Assistant, Department of Aerospace Engineering and Mechanics, AIAA student member
†Professor, Department of Aerospace Engineering and Mechanics, 110 Union ST SE, AIAA Fellow.

improved performance for incompressible flows.[7,8] Therefore, we develop a compressible version of the DSM model with SGS KE equation. The SGS KE transport equation for compressible flow is derived, and the unclosed terms in the compressible KE equation are modeled and dynamically closed using the Germano's identity. The proposed model is incorporated with the parallel finite volume Navier-Stokes solver on unstructured grids developed by Park & Mahesh[6] (2007) and applied to decaying isotropic turbulence and normal shock/isotropic turbulence interaction.

# II. LES Modeling Background

LES is based on the concept of decomposing flow variables into the resolved (filtered) terms and the subgrid scale (residual) ones. For example, any flow variable can be decomposed as

$$\phi\left(x\right) = \bar{\phi}\left(x\right) + \phi'\left(x\right) \tag{1}$$

where,

$$\bar{\phi}\left(x\right) = \int_{\Omega} G_{\Delta}\left(x,y\right)\phi\left(y\right)dy \tag{2}$$

denotes the spatial filtering of $\phi\left(x\right)$. $G_{\Delta}\left(x,y\right)$ is called the kernel of the filter which satisfies the normalization condition

$$\int_{\Omega} G_{\Delta}\left(x,y\right)dy = 1. \tag{3}$$

In practice, the filter is usually the grid filter with unknown filter width $\Delta$ and kernel $G$, especially for unstructured grids. The filtered quantities are solved numerically from the filtered governing equations, which provides an approximation to the large-scale motions in the flow fields. Within the filtered governing equations, there are subgrid scale stress terms representing the influence of subgrid scale motions on the resolved field. These subgrid scale terms can not be calculated directly and thus are modeled in terms of resolved quantities, for closure.

## A. The Filtered Navier-Stokes Equations

For compressible flow, the density weighted (Favre) filtering is applied, i.e., for any quantities, the Favre-filtering is defined as

$$\tilde{\phi} = \frac{\overline{\rho\phi}}{\bar{\rho}}. \tag{4}$$

When Favre-filtered, the spatially filtered compressible Navier-Stokes equations take the form of

$$\begin{aligned}
\frac{\partial\bar{\rho}}{\partial t} &= -\frac{\partial\left(\bar{\rho}\widetilde{u_j}\right)}{\partial x_j}, \\
\frac{\partial\left(\bar{\rho}\widetilde{u_i}\right)}{\partial t} &= -\frac{\partial}{\partial x_j}\left(\bar{\rho}\widetilde{u_i}\widetilde{u_j} + \bar{p}\delta_{ij} - \widetilde{\sigma_{ij}} + \tau_{ij}\right), && (5)\\
\frac{\partial}{\partial t}\left(\bar{\rho}\widetilde{E}\right) &= -\frac{\partial}{\partial x_j}\left(\bar{\rho}\widetilde{E}\widetilde{u_j} + \bar{p}\widetilde{u_j} - \widetilde{\sigma_{ij}}\widetilde{u_i} - \overline{Q_j} + q_j\right) + H, && (6)\\
\bar{p} &= \bar{\rho}R\widetilde{T}
\end{aligned}$$

where $\rho$, $u_i$, $p$, $E$ are density, velocity, pressure and specific total energy, respectively. The viscous stress $\widetilde{\sigma_{ij}}$ and heat flux $\overline{Q_j}$ are given by

$$\widetilde{\sigma_{ij}} = \mu\left(\frac{\partial\widetilde{u_i}}{\partial x_j} + \frac{\partial\widetilde{u_j}}{\partial x_i} - \frac{2}{3}\frac{\partial\widetilde{u_k}}{\partial x_k}\delta_{ij}\right), \quad (7)$$

$$\overline{Q_j} = \kappa\frac{\partial\widetilde{T}}{\partial x_j} \quad (8)$$

here $\mu$ is the molecular viscosity and $\kappa$ is the thermal conductivity. And

$$\tau_{ij} = \bar{\rho}\left(\widetilde{u_i u_j} - \widetilde{u_i}\widetilde{u_j}\right), \quad (9)$$

$$q_j = C_p\left(\overline{\rho T u_j} - \bar{\rho}\widetilde{T}\widetilde{u_j}\right), \quad (10)$$

are the SGS stress and SGS heat flux, respectively. The expression for $H$ in equation (6) is

$$\begin{aligned} H = & \frac{\partial}{\partial x_j}\left[\frac{1}{2}\left(\bar{\rho}\widetilde{u_i u_i}\tilde{u_j} - \bar{\rho}\widetilde{u_i u_i u_j}\right)\right] + \frac{\partial}{\partial x_j}\left[\tilde{\mu}\frac{\partial k}{\partial x_j}\right] + \left[\overline{\mu\frac{\partial u_i}{\partial x_j}\frac{\partial u_j}{\partial x_i}} - \tilde{\mu}\frac{\partial\tilde{u}_i}{\partial x_j}\frac{\partial\tilde{u}_j}{\partial x_i}\right] \\ & + \frac{\partial}{\partial x_j}\left[\frac{1}{3}\left(\overline{\mu u_j\frac{\partial u_k}{\partial x_k}} - \tilde{\mu}\tilde{u_j}\frac{\partial\tilde{u_k}}{\partial\tilde{x_k}}\right)\right] - \left[\overline{\mu\left(\frac{\partial u_k}{\partial x_k}\right)^2} - \tilde{\mu}\left(\frac{\partial\tilde{u_k}}{\partial x_k}\right)^2\right] \end{aligned} \quad (11)$$

where, $k$ in equation (11) is the SGS kinetic energy defined by

$$\bar{\rho}k = \frac{1}{2}\tau_{kk} = \frac{1}{2}\bar{\rho}\left(\widetilde{u_k u_k} - \tilde{u_k}\tilde{u_k}\right). \quad (12)$$

Several assumptions have been made to derive the above equations. Firstly, the filtering operations and derivatives are assumed to be commutable. Secondly, the viscosity $\mu$ and thermal conductivity $\kappa$ are insensitive to filters of different levels, and are taken out of the filtering operations.

All of the SGS stress, SGS heat flux and most of the terms in equation (11) can not be computed directly from the resolved quantities. Models for these terms are discussed below.

### B. Dynamic Smagorinsky Model (DSM)

In the compressible version of DSM, the $H$ term defined by equation (11) is omitted. The SGS stress and SGS heat flux terms are modeled by

$$\tau_{ij} - \frac{\delta_{ij}}{3}\tau_{kk} = -2C_s\bar{\rho}\Delta^2|\widetilde{S}|\widetilde{S_{ij}^*} \quad (13)$$

$$q_j = -\bar{\rho}\frac{C_s\Delta^2|\widetilde{S}|}{Pr_T}\frac{\partial\bar{T}}{\partial x_j} \quad (14)$$

and Yoshizawa's formula is used to model $\tau_{kk}$ or SGS kinetic energy, $k$, effectively. Namely,

$$\tau_{kk} = 2C_I\bar{\rho}\Delta^2|\widetilde{S}|^2 \quad (15)$$

where $|S| = \sqrt{2S_{ij}S_{ij}}$ and $S_{ij}^* = S_{ij} - \frac{1}{3}S_{kk}\delta_{ij}$. Model coefficients $C_s$, $C_I$, $Pr_T$ are determined dynamically by the Germano identity, which assumes similarities of SGS quantities between the grid filter level and test filter level. To be exact, for any terms that take the form of $a = \overline{\alpha\beta} - \bar{\alpha}\bar{\beta}$, we assume that, on the test filter level, $A = \widehat{\overline{\alpha\beta}} - \widehat{\bar{\alpha}}\widehat{\bar{\beta}}$ holds. The Germano identity is then defined by $L = A - \hat{a} = \widehat{\bar{\alpha}\bar{\beta}} - \widehat{\bar{\alpha}}\widehat{\bar{\beta}}$, which can be calculated from the resolved variables. Assume the model for $a$ is $a = C \cdot m$, where $m$ is a function of the resolved (grid filter level) quantities; then in the test filter level, $A = C \cdot M$, where $M$ takes similar form as $m$ but is a function of the test-filtered quantities. Plug in the models for $A$ and $a$, Germano identity becomes

$$L = \widehat{\bar{\alpha}\bar{\beta}} - \widehat{\bar{\alpha}}\widehat{\bar{\beta}} = C\left(M - \hat{m}\right). \quad (16)$$

Both sides of equation (16) are directly calculable from the resolved variables, thus the model coefficient $C$ can be solved dynamically as

$$C = \frac{\widehat{\bar{\alpha}\bar{\beta}} - \hat{\bar{\alpha}}\hat{\bar{\beta}}}{(M - \hat{m})}, \tag{17}$$

making $C$ adaptable to time and space. Finally, to avoid computational instability, $C$ is regularized using a combination of least-square[10] and volume averaging, e.g. the formula for the model coefficient of SGS stress $C_s$ is

$$C_s \Delta^2 = \frac{1}{2} \frac{\left\langle L_{ij}^* M_{ij}^* \right\rangle}{\left\langle M_{ij}^* M_{ij}^* \right\rangle}$$

where

$$\begin{aligned} L_{ij} &= \left( \frac{\widehat{\overline{\rho u_i}\, \overline{\rho u_j}}}{\bar{\rho}} \right) - \frac{\widehat{\overline{\rho u_i}}\, \widehat{\overline{\rho u_j}}}{\hat{\bar{\rho}}} \\ L_{ij}^* &= L_{ij} - L_{kk}\delta_{ij} \\ M_{ij}^* &= \bar{\rho} \widehat{|\widetilde{S}\widetilde{S}_{ij}^*|} - \hat{\bar{\rho}} \left( \frac{\widehat{\Delta}}{\Delta} \right)^2 |\widehat{\widetilde{S}}| \widehat{\widetilde{S}_{ij}^*}. \end{aligned} \tag{18}$$

Here, $\langle \cdot \rangle$ denotes spatial average over homogeneous directions and $\widehat{\cdot}$ denotes the test filtering. For the formula of $Pr_t$ in the SGS heat flux $q_j$ and any other details about the compressible DSM please refer to Moin *et al.*'s work.[3]

## III. Dynamic SGS k-Equation Model

Instead of using Yoshizawa's model (Eq. (15)) for SGS KE, its transport equation is introduced in the dynamic SGS k-equation model. It has been shown[7,8] that DSM with SGS k-equation model gives better performance in LES of incompressible flows. Thus, we extend this idea to compressible flows. Consider the SGS KE transport equation first.

### A. SGS KE Transport Equation

The SGS KE equation can be derived by subtracting the product of filtered velocity and the filtered momentum equation from the filtered product of velocity and momentum equation, i.e.,

$$[u_i \times (\widetilde{momentum\ equation})] - \widetilde{u}_i \times (\widetilde{momentum\ equation})$$

After reduction and rearrangement of the above equation, the SGS KE equation can be obtained as

$$
\begin{aligned}
\frac{\partial \bar{\rho} k}{\partial t} &= -\frac{\partial \bar{\rho} k \tilde{u_j}}{\partial x_j} - R\frac{\partial q_j}{\partial x_j} + \frac{\partial \tau_{ij}\tilde{u_i}}{\partial x_j} - \tau_{ij}\widetilde{S_{ij}} + \frac{\partial}{\partial x_j}\left[\tilde{\mu}\frac{\partial k}{\partial x_j}\right] \\
&+ \frac{\partial}{\partial x_j}\left[\frac{1}{2}\bar{\rho}\left(\widetilde{u_i u_i}\tilde{u_j} - \widetilde{u_i u_i u_j}\right) + \frac{1}{3}\left(\overline{\mu u_j \frac{\partial u_k}{\partial x_k}} - \tilde{\mu}\tilde{u_j}\frac{\partial \tilde{u_k}}{\partial \tilde{x_k}}\right)\right] \\
&- \left(\overline{\mu \frac{\partial u_i}{\partial x_j}\frac{\partial u_i}{\partial x_j}} - \tilde{\mu}\frac{\partial \tilde{u_i}}{\partial x_j}\frac{\partial \tilde{u_i}}{\partial x_j}\right) - \frac{1}{3}\left[\overline{\mu\left(\frac{\partial u_k}{\partial x_k}\right)^2} - \tilde{\mu}\left(\frac{\partial \tilde{u_k}}{\partial x_k}\right)^2\right] . \qquad (19) \\
&+ \left(\overline{p\frac{\partial u_k}{\partial x_k}} - \bar{p}\frac{\partial \tilde{u_k}}{\partial x_k}\right) + \frac{\partial}{\partial x_j}\left[\overline{\mu\frac{\partial\left(\frac{1}{2}u_i u_i\right)}{\partial x_j}} - \tilde{\mu}\frac{\partial\left(\frac{1}{2}\widetilde{u_i u_i}\right)}{\partial x_j}\right] \\
&+ \left[\overline{\left(u_i\frac{\partial u_j}{\partial x_i} - u_j\frac{\partial u_k}{\partial x_k}\right)\frac{\partial \mu}{\partial x_j}} - \left(\tilde{u_i}\frac{\partial \tilde{u_j}}{\partial x_i} - \tilde{u_j}\frac{\partial \tilde{u_k}}{\partial x_k}\right)\frac{\partial \tilde{\mu}}{\partial x_j}\right]
\end{aligned}
$$

where $k$, $\tau_{ij}$, $q_j$ are SGS kinetic energy, SGS stress and SGS heat flux defined by equation (12), (9) and (10), respectively. $S_{ij}$ is rate of strain tensor. Equation (19) is the exact form of the SGS KE equation. The only assumption has been made is the commutability of derivative and filtering operations. For simplicity, the last two terms are neglected. The resulting SGS KE equation is

$$
\begin{aligned}
\frac{\partial \bar{\rho} k}{\partial t} &= -\frac{\partial \bar{\rho} k \tilde{u_j}}{\partial x_j} - R\frac{\partial q_j}{\partial x_j} + \frac{\partial \tau_{ij}\tilde{u_i}}{\partial x_j} - \tau_{ij}\widetilde{S_{ij}} + \frac{\partial}{\partial x_j}\left[\tilde{\mu}\frac{\partial k}{\partial x_j}\right] \\
&+ \frac{\partial f_j}{\partial x_j} - \epsilon_s - \epsilon_c + \Pi
\end{aligned} \qquad (20)
$$

where

$$
f_j = \frac{1}{2}\bar{\rho}\left(\widetilde{u_i u_i}\tilde{u_j} - \widetilde{u_i u_i u_j}\right) + \frac{1}{3}\left(\overline{\mu u_j \frac{\partial u_k}{\partial x_k}} - \tilde{\mu}\tilde{u_j}\frac{\partial \tilde{u_k}}{\partial \tilde{x_k}}\right), \qquad (21)
$$

$$
\epsilon_s = \overline{\mu\frac{\partial u_i}{\partial x_j}\frac{\partial u_i}{\partial x_j}} - \tilde{\mu}\frac{\partial \tilde{u_i}}{\partial x_j}\frac{\partial \tilde{u_i}}{\partial x_j}, \qquad (22)
$$

$$
\epsilon_c = \frac{1}{3}\left[\overline{\mu\left(\frac{\partial u_k}{\partial x_k}\right)^2} - \tilde{\mu}\left(\frac{\partial \tilde{u_k}}{\partial x_k}\right)^2\right], \qquad (23)
$$

$$
\Pi = \overline{p\frac{\partial u_k}{\partial x_k}} - \bar{p}\frac{\partial \tilde{u_k}}{\partial x_k}, \qquad (24)
$$

are transport (triple correlation + dilatational diffusion), SGS dissipation, dilatational dissipation, pressure dilatation terms. These terms are to be modeled for closure.

## B. Residual Term H in Filtered Total Energy Equation

In almost all of the LES modeling of compressible flows, the residual term $H$ in the filtered energy equation (6) is omitted, partially because there are too many unclosed terms in $H$ adding the complexity of modeling. However, for the SGS k-equation model, we can take into account all of the terms of $H$ without adding extra computation and modeling cost. Recall equation (11) for the expression of $H$,

$$H = \frac{\partial}{\partial x_j}\left[\frac{1}{2}\left(\bar{\rho}\widetilde{u_i u_i}\tilde{u_j} - \bar{\rho}\widetilde{u_i u_i u_j}\right)\right] + \frac{\partial}{\partial x_j}\left[\tilde{\mu}\frac{\partial k}{\partial x_j}\right] + \left[\overline{\mu\frac{\partial u_i}{\partial x_j}\frac{\partial u_j}{\partial x_i}} - \tilde{\mu}\frac{\partial \tilde{u_i}}{\partial x_j}\frac{\partial \tilde{u_j}}{\partial x_i}\right]$$

$$+\frac{\partial}{\partial x_j}\left[\frac{1}{3}\left(\overline{\mu u_j\frac{\partial u_k}{\partial x_k}} - \tilde{\mu}\tilde{u_j}\frac{\partial \tilde{u_k}}{\partial \tilde{x_k}}\right)\right] - \left[\overline{\mu\left(\frac{\partial u_k}{\partial x_k}\right)^2} - \tilde{\mu}\left(\frac{\partial \tilde{u_k}}{\partial x_k}\right)^2\right].$$

$H$ has a lot of terms common with the SGS KE tranport equation (20). All terms, except the third one,

$$\epsilon^* = \overline{\mu\frac{\partial u_i}{\partial x_j}\frac{\partial u_j}{\partial x_i}} - \tilde{\mu}\frac{\partial \tilde{u_i}}{\partial x_j}\frac{\partial \tilde{u_j}}{\partial x_i}, \tag{25}$$

reappear in the SGS KE transport equation. Note that $\epsilon^*$ has very similar form as $\epsilon_s$ in equation (22), and will be modeled similarly. The filtered total energy equation can be re-written as

$$\frac{\partial}{\partial t}\left(\bar{\rho}\widetilde{E}\right) = -\frac{\partial}{\partial x_j}\left(\bar{\rho}\widetilde{E}\tilde{u_j} + \bar{p}\tilde{u_j} - \widetilde{\sigma_{ij}}\tilde{u_i} - \overline{Q_j} + q_j\right) + \frac{\partial}{\partial x_j}\left[\tilde{\mu}\frac{\partial k}{\partial x_j}\right] + \frac{\partial f_j}{\partial x_j} - \epsilon^* - 3\epsilon_c \tag{26}$$

## C. SGS Modeling

Similar to the standard dynamic Smagorinsky model, eddy viscosity and eddy diffusivity models are used for the SGS tress $\tau_{ij}$ and the SGS heat flux $q_j$, respectively. However, with the SGS KE equation, $\sqrt{k}$ is chosen as the velocity scale instead of $\Delta|\widetilde{S}|$, i.e.

$$\tau_{ij} - \frac{2}{3}\bar{\rho}k\delta_{ij} = -2C_s\Delta\bar{\rho}\sqrt{k}\left(\widetilde{S_{ij}} - \frac{1}{3}\widetilde{S_{kk}}\delta_{ij}\right), \tag{27}$$

$$q_j = -\frac{\mu_t}{Pr_t}\frac{\partial \widetilde{T}}{\partial x_j} = -\frac{C_s\Delta\bar{\rho}\sqrt{k}}{Pr_t}\frac{\partial \widetilde{T}}{\partial x_j}. \tag{28}$$

Here, again, $C_s$ and $Pr_t$ are the model coefficients that are determined dynamically by Germano's identity. The closure of energy equations requires models for $f_j$, $\epsilon_s$, $\epsilon^*$, $\epsilon_c$ and $\Pi$. We propose the following models for these terms.

$$f_j = C_f\bar{\rho}\Delta\sqrt{k}\frac{\partial k}{\partial x_j}, \tag{29}$$

$$\epsilon_s = C_{\epsilon s}\bar{\rho}k^{3/2}\Delta^{-1}, \tag{30}$$

$$\epsilon^* = C_{\epsilon *}\bar{\rho}k^{3/2}\Delta^{-1}, \tag{31}$$

$$\epsilon_c = C_{\epsilon c}M_t^2\bar{\rho}k^{3/2}\Delta^{-1}, \tag{32}$$

$$\Pi = C_\Pi\Delta^2\frac{\partial \bar{p}}{\partial x_j}\frac{\partial^2\widetilde{u_k}}{\partial x_j\partial x_k} \tag{33}$$

where $C_f$, $C_{\epsilon s}$, $C_{\epsilon *}$, $C_{\epsilon c}$, $C_\Pi$ are closure coefficients to be determined dynamically; $\Delta$ is the nominal filter width; $M_t = \frac{\sqrt{2k}}{a}$ is the SGS turbulent Mach number, where $a$ is the mean speed of sound. The above models mostly originate from RANS models for turbulent kinetic energy. Models for $f_j$, $\epsilon_s$ are adapted from the models of corresponding terms for incompressible SGS KE equations,[7] while $\epsilon^*$ is modeled analogously to $\epsilon_s$. Model for dilatational dissipation term $\epsilon_c$ is from Sakar *et al.*,[11,12] and the model for pressure dilatational term $\Pi$ is based on series expansion. For any term that has the structure of $\overline{fg} - \bar{f}\bar{g}$, on a uniform grid ($dx = dy = dz$), Bedford and Yeo[13] show that

$$\begin{aligned}\overline{fg} - \bar{f}\bar{g} &= 2\alpha \frac{\partial \bar{f}}{\partial x_k}\frac{\partial \bar{g}}{\partial x_k} + \frac{1}{2!}(2\alpha)^2 \frac{\partial^2 \bar{f}}{\partial x_k \partial x_l}\frac{\partial^2 \bar{g}}{\partial x_k \partial x_l} \\ &+ \frac{1}{3!}(2\alpha)^2 \frac{\partial^3 \bar{f}}{\partial x_k \partial x_l \partial x_m}\frac{\partial^2 \bar{g}}{\partial x_k \partial x_l \partial x_m} + ...\end{aligned} \tag{34}$$

where

$$\alpha(y) = \int_{-\infty}^{\infty} x^2 G(x,y)\, dx \tag{35}$$

and $G(x,y)$ is the kernel of the filter. For a box filter, $\alpha = \Delta^2/24$. In practice, $\alpha$ is approximated by $\alpha = C\Delta^2$, and $C$ is absorbed in the model coefficient $C_\Pi$.

Most of the model coefficients can be dynamically computed through Germano identity. The detailed formulations are omitted here, please refer to section II - B for the generalized procedures. However, since the model for SGS dissipation $\epsilon_s$ does not scale well across filters, the Germano identity for $\epsilon_s$ yields very small values of $C_{\epsilon s}$ which considerably under-predicts the magnitude of $\epsilon_s$ causing incorrect evolution of SGS kinetic energy. To circumvent this problem, instead of using Germano identity, which assumes similarity of SGS stresses between the grid filter level and the test filter level, we use the analogy between the grid-filter-level SGS stress and Leonard stress $L_{ij}$ across the test filter level.[8] Specifically, in Germano identity, the SGS stress in the test filter level is assumed to be

$$T_{ij} = \widehat{\overline{u_i u_j}} - \widehat{\bar{u}_i}\,\widehat{\bar{u}_j}\ . \tag{36}$$

However, Menon *et al.* use

$$T_{ij} = \widehat{\bar{u}_i\,\bar{u}_j} - \widehat{\bar{u}_i}\,\widehat{\bar{u}_j}\ , \tag{37}$$

which is the Leonard term $L_{ij}$ in Germano identity. The counterpart of $L_{ij}$ for compressible flow is defined by equation (18). We apply similar dynamic procedures to the calculation of coefficient $C_{\epsilon s}$ in the model of $\epsilon_s$, and obtain reasonable values of $C_{\epsilon s}$ and correct decaying rate of SGS kinetic energy of temporal decaying isotropic turbulence. Note that this method is only for $C_{\epsilon s}$ and $C_{\epsilon *}$, the Germano identity is used for all the other terms.

# IV. Results and Discussion

The dynamic SGS k-equation model is incorporated into the parallel finite volume Navier-Stokes solver on unstructured grids developed by Park & Mahesh[6] (2007) and applied to decaying isotropic turbulence and normal shock/isotropic turbulence interaction problems.

## A. Decaying Isotropic Turbulence

Spatial averaging over homogeneous directions are applied during the dynamic procedures. Two cases are considered here, both of which are simulated on a $32^3$ periodic cubical domain.

*Case 1:*

The initial spectrum obeys

$$E(k) = 16\sqrt{\frac{2}{\pi}}\frac{u_0^2}{k_0}\left(\frac{k}{k_0}\right)^4 exp\left(-2k^2/k_0^2\right) \tag{38}$$

where $k_0 = 5$ and $u_0 = 1$. The initial micro-scale Reynolds number $Re_\lambda = u_{rms}\lambda/\nu = 100$, where $\lambda$ is the Taylor microscale. The initial turbulent Mach number is set to be $M_t = 0.1$. The initial condition for SGS kinetic energy is calculated from Yoshizawa's model. Figure 1 compares the total kinetic energy decay and

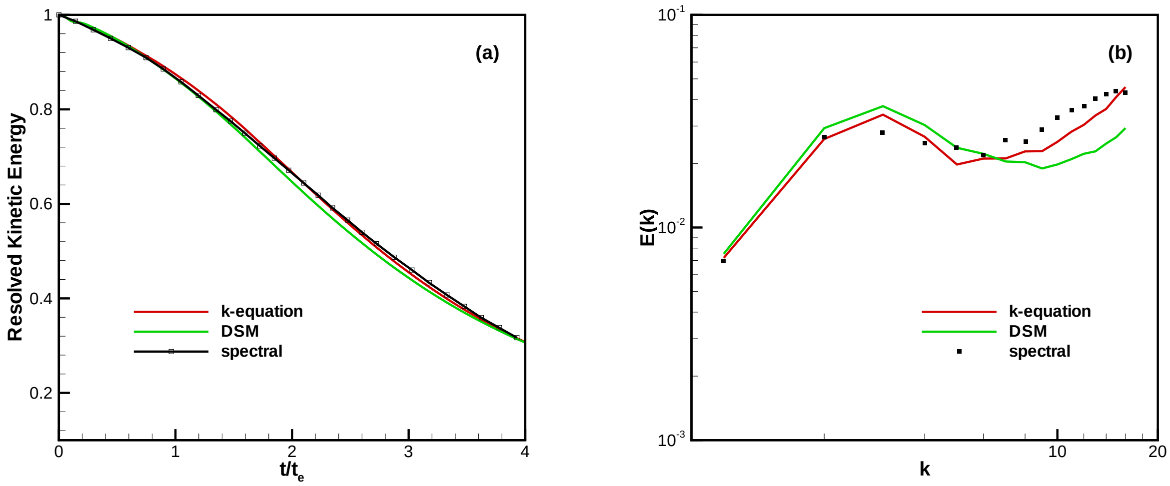


**Figure 1. Resolved total energy decay $(a)$ and energy spectrum $(b)$ at $t = 4t_e$.**

the energy spectrum at time $t = 4t_e$ from k-equation model with those from compressible DSM and dealiased pseudo-spectral code for incompressible flow. Here, $t_e$ is the eddy turn-over time defined as $t_e = \lambda/u_{rms}$. In the figure the resolved kinetic energy is normalized with its initial value, while the time is scaled with the eddy turn-over time $t_e$.

The new dynamic k-equation model shows slightly better result than DSM which is known to be a good model for decaying isotropic turbulence problems. Since Yoshizawa's model under-predict the SGS kinetic energy which is taken as the initial value for k-equation, at the beginning, the dynamic k-equation model gives slightly slower decay rate of KE due to lower eddy viscosity modeled through the under-predicted SGS KE. Afterwards, the SGS KE adapts to the correct value and the decay rate of the resolve kinetic energy agrees well with the pseudo spectral code results.

*Case 2: CBC*

Comte-Bellot & Corrsin's[9] (CBC) experiment is simulated with dynamic k-equation model. The initial spectrum is obtained from the experimental data. SGS KE is again initialized with the help of DSM, however, the magnitude is scaled so that the mean value of SGS KE matches the experimental SGS KE which can be estimated by integrating the energy spectrum over wave numbers that are higher than the cutoff wave number. The performance of the proposed dynamic k-equation model are compared with that of standard DSM and the experimental data in figure 2, where figure 2 $(a)$ shows the temporal decay of kinetic energy, while figure 2 $(b)$ shows the energy spectrum at different time instances which correspond to the three different locations of $U_0t/M = 42, 98, 171$ in CBC experiment. As shown in figure 2, the results from the new dynamic k-equation model is very encouraging that the kinetic energy decay, especially the SGS KE, agree with the experiment better than DSM. The cusp of energy spectrum is reduced and postponed to higher wave numbers by the dynamic k-equation model, too. Again, Yoshizawa's Model in DSM under-predicts the SGS KE.

### B. Normal Shock/Isotropic Turbulence Interaction

The schematic of the problem is shown in figure 3. Isotropic turbulence is introduced at the inflow, decays spatially over a short distance then interacts with a statistically stationary normal shock. A sponge layer is used at the end of the computational domain to absorb reflected acoustic oscillations. Spatial averaging

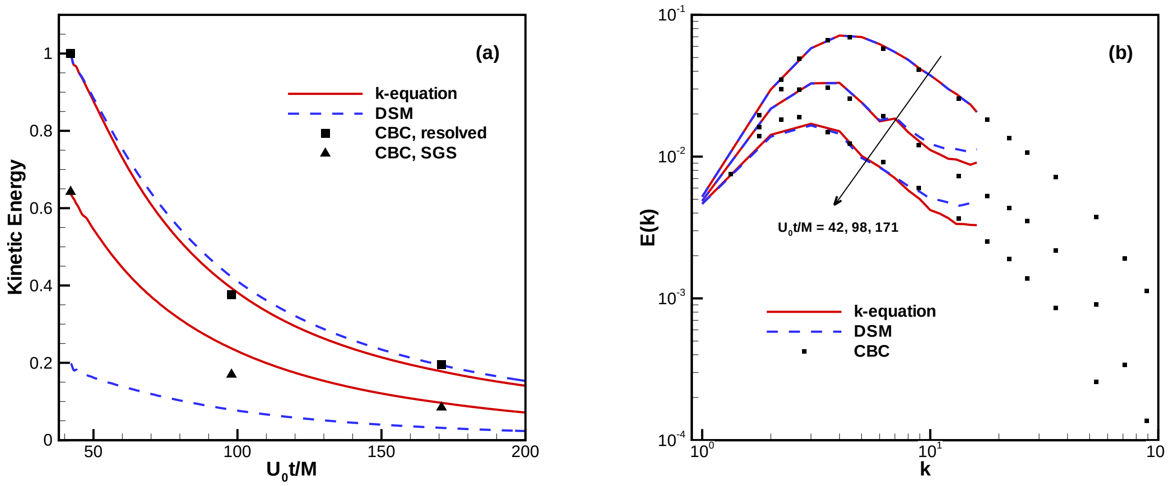


**Figure 2. LES with k-equation model and DSM model for the CBC decaying isotropic turbulence on $32^3$ resolution.**

over homogeneous directions ($y - z$ planes) is applied during the dynamic procedures.

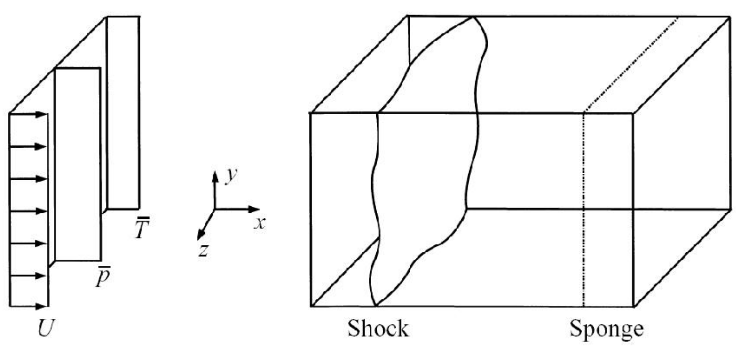


**Figure 3. Schematic of shock/turbulence interaction problem.**

Again, two cases are considered here. The first case has low $Re$ which corresponds to Mahesh it et al.'s[14] DNS, where the inflow Mach number is $M = 1.29$, the turbulent Mach number of the inflow is $M_t = 0.14$, and the micro-scale Reynolds number is $Re_\lambda = 19.1$. The second case corresponds to Larsson's[15] DNS, which has higher $Re$, freestream Mach number $M$ and turbulent Mach number $M_t$ ($M = 1.5$, $M_t = 0.221$, $Re_\lambda = 40.0$). The two simulations are carried out on the same computation domain with exactly the same mesh. The domain has the dimension of $L_x = 10$ in streamwise direction, $L_y = L_z = 2\pi$ in the transverse directions. The mesh has $180 \times 32^2$ CVs, which is uniform in the transverse directions and clustered in the vicinity of the shock in streamwise direction.

The inflow isotropic turbulence are generated using similar method as Mahesh *et al*'s. An isotropic turbulence, which has the initial energy spectrum of equation (38), is allowed to decay temporally until the designated $M_t$ and $Re_\lambda$ are reached. Then, the snapshot of the flow field is taken and used as the inflow of shock/turbulent interaction problem based on Taylor's hypothesis. However, since the length of the domain, $L_x$, for shock/turbulent interaction is larger than the width, $L_z$, and the height, $L_y$, the simulation of the isotropic turbulence is performed on a uniformly meshed long periodic box which has the dimension of $n\pi \times 2\pi \times 2\pi$ (figure 4), to avoid periodic input of inflow information. $n$ is chosen big enough to generate inflow data sequence that is long enough to provide unduplicated isotropic inflow turbulence for several flow-over time, so that converged statistics can be achieved. For current case, $n$ is thus chosen as 16, which will provide around 5 flow-over time of inflow data and is proven to be enough for the statistics to converge. This methodology is validated by temporally and spatially decaying isotropic turbulence as shown in figure 5, where ($a$) compares the temporal decay of kinetic energy for isotropic turbulence in a periodic cube and a long periodic box, starting with the same energy spectrum. Figure 5 ($b$) compares the energy decay rate of the temporally decaying isotropic turbulence and the spatially decaying one where the inflow isotropic turbulence is extracted from the temporal case at time $t/t_e = 1.58$. Good agreement is observed for both cases. Then, the isotropic turbulent inflow is allowed to convect into the computational domain of shock/turbulence interaction.

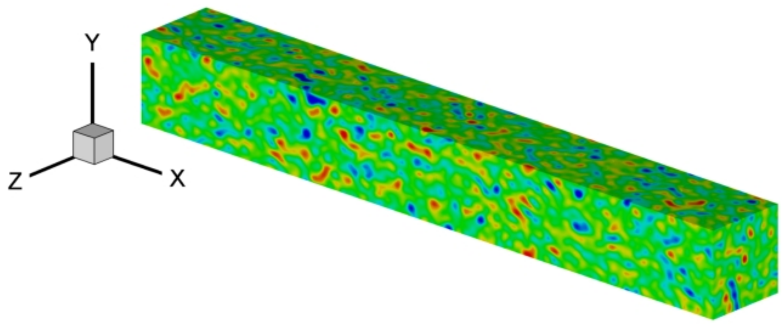


**Figure 4. Decaying isotropic turbulence in long periodic box.**

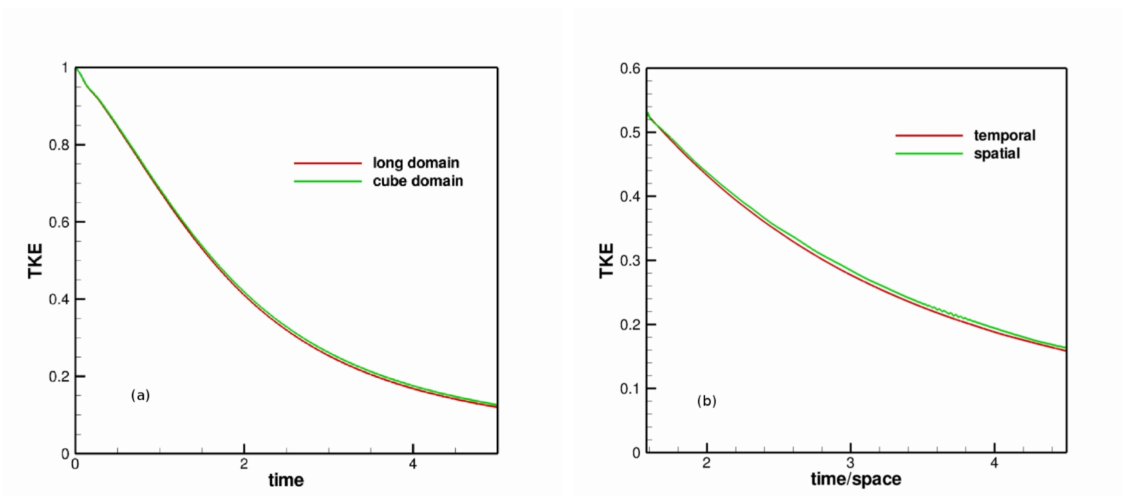


**Figure 5. Validation of inflow turbulence generation and implementation.**

### *1. Low Re case*

Figure 6 compares the distribution of averaged turbulent intensities calculated from the k-equation model and the standard DSM model with DNS results. In figure 6 ($a$) and ($b$), the resolved and the SGS turbulent intensities are normalized by the values of the resolved one immediately upstream of the shock, to compare with the DNS results.[14] Here, the SGS turbulent intensities are estimated based on the hypothesis of eddy

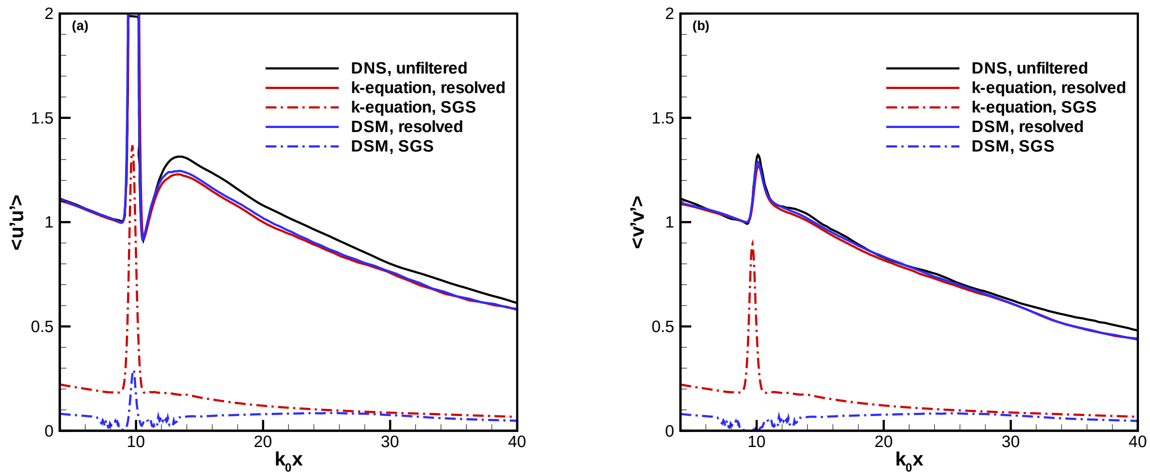


**Figure 6. Distribution of averaged turbulent intensities. All curves have been normalized by their values immediately upstream of the shock.**

viscosity and the analogy between the Reynolds stress in the RANS equation and the average SGS stress in the time-averaged filtered momentum equation, i.e.,

$$\langle u_i' u_j' \rangle_{SGS} = \left\langle 2\mu_t \widetilde{S_{ij}^*} + \frac{2}{3}\delta_{ij} k \right\rangle . \tag{39}$$

Here, $\widetilde{S_{ij}^*}$ has the same expression as in equation (13), $k$ is the SGS kinetic energy, and $\langle . \rangle$ denotes the ensemble averaging. For shock/turbulence interaction problem, $\widetilde{S_{ij}^*}$ is very small, so the SGS intensities are dominated by the second term in equation (39), and hence is a good representation of SGS kinetic energy. Thus, the evolution of the SGS kinetic energy is not plotted here. As shown in figure 6, both of the DSM and k-equation model predict $\langle v'v' \rangle$ very well, while both under-predict $\langle u'u' \rangle$ a little compared to the unfiltered DNS result. In terms of the resolved turbulent intensities, the difference between the DSM results and that of k-equation model are almost indiscernible for current simulation. However, the SGS scale turbulent intensities differ a lot. In DSM model, the magnitude of SGS turbulent intensities (or kinetic energy) is smaller with random oscillations in the vicinity of the shock and becomes larger on both windward and leeward sides of the shock. This is because Yoshizawa's model used in the standard DSM does not take into account the history of the SGS kinetic energy, which make it more sensitive to the grid resolution. Intuitively, the coarser the grid the higher the SGS KE, and vice verse. The distribution pattern of the SGS KE from the DSM model is the joint effect of clustering mesh near the shock and the spatial decaying of SGS KE. The dynamic k-equation model circumvents this problem by using SGS KE transport equation and yields more reasonable evolution of SGS turbulent intensities across the shock, where the SGS turbulent intensities jump across the shock, then decay spatially afterwards.

*2. High Re case*

Figure 7 shows the comparisons of the distribution of averaged turbulent strength calculated from the k-equation model, the standard DSM model and DNS of Larsson. Different from the low Reynolds number case, the difference between the k-equation model and DSM calculation of the resolved turbulent intensities is noticeable. Note that the k-equation model is closer to the unfiltered DNS over both the near and the far field. Interestingly, the DSM predicts higher values than unfiltered DNS in the far field. Again, the evolution of SGS KE is more reasonably predicted by k-equation model. However, the behavior of SGS KE is a lot different from the low Reynolds number case(figure 6). The magnitude of the jump of SGS KE within the shock is further intensified for high *Re* flow, while the SGS KE does not relax as quickly as the low *Re* case.

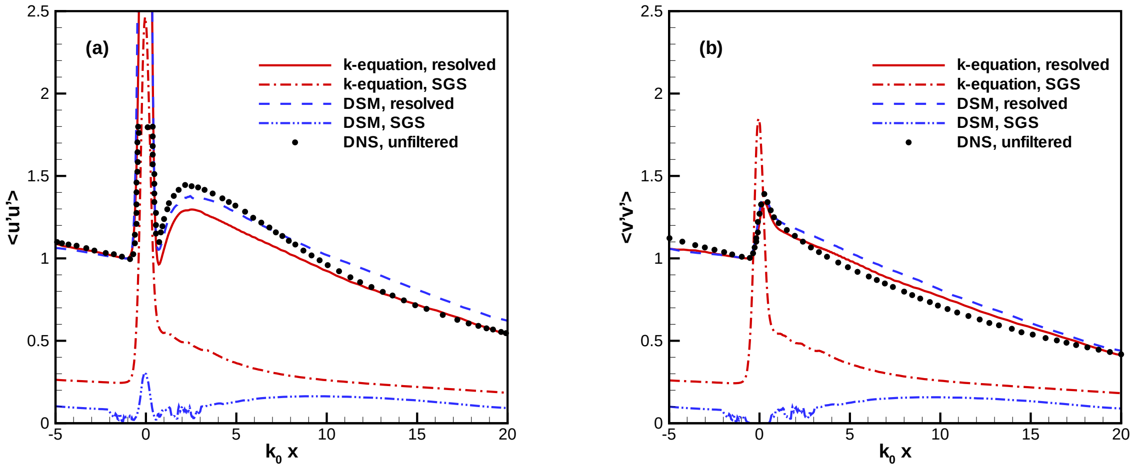


**Figure 7. Distribution of averaged turbulent intensities. All curves are normalized by their values immediately upstream of the shock. The shock position has been shifted to $x = 0$ for comparison with DNS of Larsson.**

The new dynamic k-equation model has another advantage: it is stable during the use of local averaging over the neighboring CVs for the dynamic procedures, while the DSM model is not. Figure 8 compares the results of k-equation model derived from local averaging and averaging over homogeneous directions. The difference is indiscernible until far downstream of the shock, where the local averaging gives slower decay rate of turbulent intensities. Similar under-predictions of decay rate of kinetic energy are also observed in simulations of temporal and spatial decaying isotropic turbulence using local averaging, Such localization of the dynamic k-equation model facilitates its application to simulations of complex flow fields on unstructured grids.

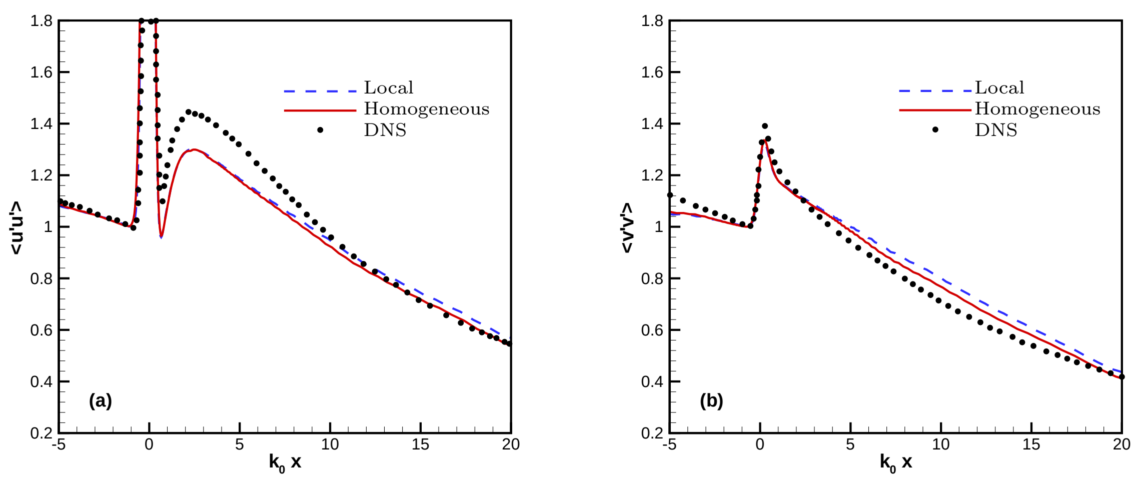


**Figure 8. Comparison of local averaging and averaging over homogeneous directions.**

## V. Conclusions

A new dynamic Smagorinsky model with SGS kinetic energy equation for compressible LES is proposed. The SGS kinetic energy transport equation is derived, and the residual terms in the filtered total energy equation that are omitted by previous works have been revisited. The unclosed terms in the filtered governing equations and the SGS k-equation are modeled, and the model coefficients are determined dynamically. A new algebraic model based on series expansion is proposed for the pressure dilatation term. A different dynamic procedure for SGS dissipation model is suggested and proven to work well. The new k-equation model is incorporated into a parellel finite volume Navier-Stokes solver on unstructured grids[6] and successfully applied to the decaying isotropic turbulence and isotropic turbulence and normal shock interaction problems. Compared with available experimental and DNS results, current LES results show great agreements for both problems. The proposed the k-equation model outperforms the standard DSM model in the simulations of general turbulence flows by giving better prediction of resolved variables and much more accurate estimation of SGS quantities. In addition, compared with DSM, k-equation model also has the feature of easy localization, even for challenging problems, which will facilitate its application to the flow field with complex geometries as well as N-S solvers on unstructured grids.

## Acknowledgments

This work is supported by the National Science Foundation under grant CTS–0828162 and the Air Force Office of Scientific Research under grant FA9550–04–1–0341. Computer time for the simulations was provided by Minnesota Supercomputing Institute (MSI), National Institute for Computational Sciences (NICS) and Texas Advanced Computing Center (TACC). We would like to thank Dr. Noma Park for useful discussions.

## References

[1]Germano, M., Piomelli, U., Moin, P. and Cabot, M., 1991, A dynamic subgrid-scale eddy viscosity model, *Phys. Fluids A* **3**: 1760.

[2]Smagorinsky, 1963, General circulation experiments with the primitive equations. I. The basic experiment. *Mon. Weather Rev.* **91**, 99 - 165.

[3]Moin, P., Squires, K., Cabot, W. and Lee, S., 1991, A dynamic subgrid-scale model for compressible turbulence and scalar transport, *Phys. Fluids A* **3**: 2746.

[4]Yoshizawa,A., 1986 Statistical theory for compressible turbulent shear flows, with the application to subgrid modeling, *Phys. Fluids* **29**: 2152.

[5]Spyropoulos, E.T., and Blaisdell, G.A., 1996, Evaluation of the dynamic model for simulation of compressible decaying isotropic turbulence, *AIAA J.* **34**: 990.

[6]Park, N. and Mahesh, K. 2007, Numerical and modeling issues in LES of compressible turbulent flows on unstructured grids, *AIAA Paper* - 722.

[7]Ghosal, S., Lund, T. S., Moin, P. and Akselvoll, K., 1995, A dynamic localization model for large-eddy simulation of turbulent flows, *J. Fluid Mech.* **286**: 229.

[8]Menon, S., Kim, W. W., 1996, High Reynolds number flow simulations using the localized dynamic subgrid-scale model, *AIAA 34th Aerospace Sciences Meeting and Exhibit*

[9]Comte-Bellot, G. and Corrsin, S., 1971, Simple Eulerian time correalation of full- and narrow-band velocity signals in grid-generated isotropic turbulence, *J. Fluid Mech.*, **48**:273

[10]Lilly, D.K., 1991, A proposed modification of the Germano subgrid-scale closure method, *Phys. Fluids, A* **3**, 1760.

[11]Sarkar, S., Erlebacher, G., Hussaini, M. Y., and Kreiss, H. O., 1995, The analysis and modelling of dilatational terms in compressible turbulence, *J. Fluid Mech.* **227**, 473

[12]El Baz, A. M., 1992, Modelling compressibility effects on free turbulent shear flows, *5th Biennial Colloquium on Computational Fluid Dynamics*, University of Mancherster Insititute of Science and Technology, Manchester, England, U.K. 27-28. May 1992

[13]Bedford, K. W., and Yeo, W. K., 1993, Conjuctive Filtering Procesures in Surface Water Flow and Transport, *Large Eddy Simulation of Complex Engineering and Geophysical Flows*, edited by B. Galperin, and S.A. Orszag, Cambridge Univ. Press, New York, pp. 513-539

[14]Mahesh, K., LeLe, S.K., and Moin, P., 1997, The influence of entropy fluctuations on the interaction of turbulence with a shock wave, *J. Fluid Mech.*, Vol. **334**, pp. 353 - 379

[15]Larsson, J., 2008, Direct numerical simulation of canonical shock/turbulence interaction, *Center for Turbulence Research Annual Research Briefs 2008*